Ytterbium fiber laser based on first-order fiber Bragg gratings written with 400nm femtosecond pulses and a phase-mask

M. Bernier[1*], R. Vallée[1], B. Morasse[2], C. Desrosiers[2], A. Saliminia[1], and Y. Sheng[1]

[1]*Centre d'Optique, Photonique et Laser (COPL), Université Laval, Québec, Canada, G1V 0A6*
[2]*CorActive High-Tech inc., Québec, Canada, G2C 1S9*
**Martin.Bernier@copl.ulaval.ca*

Abstract: A Fiber Bragg grating of 369 *nm* pitch was inscribed in a germanium-free double-clad ytterbium doped silica fiber using a femto-second pulse train at 400 *nm* wavelength and a phase mask. The photo-induced refractive index modulation of higher than $4x10^{-3}$ was obtained and the accompanying photo-induced losses were subsequently removed by thermal annealing, resulting in a low loss (<0.1dB), stable and high reflectivity (>40dB) FBG. Based on this FBG, a monolithic Ytterbium fiber laser operating at 1073 *nm* with slope efficiency of 71% and output power of 13*W* was demonstrated.

OCIS codes: (140.3615) Lasers, Ytterbium; (230.1480) Bragg reflectors; (060.3738) Fiber Bragg gratings, photosensitivity

References and links

1. S. A. Slattery, D. N. Nikogosyan, and G. Brambilla, "Fiber Bragg grating inscription by high-intensity femtosecond UV laser light: comparison with other existing methods of fabrication," J. Opt. Soc. Am. B **22**(2), 354–361 (2005).
2. S. J. Mihailov, D. Grobnic, C. W. Smelser, P. Lu, R. B. Walker, and H. Ding, "Induced Bragg Gratings in Optical Fibers and Waveguides Using an Ultrafast Infrared Laser and a Phase Mask," Laser Chem. vol. 2008, Article ID 416251, 20 pages (2008)
3. M. Bernier, D. Faucher, R. Vallée, A. Saliminia, G. Androz, Y. Sheng, and S. L. Chin, "Bragg gratings photoinduced in ZBLAN fibers by femtosecond pulses at 800 nm," Opt. Lett. **32**(5), 454–456 (2007).
4. G. Androz, D. Faucher, M. Bernier, and R. Vallée, "Monolithic fluoride-fiber laser at 1480 nm using fiber Bragg gratings," Opt. Lett. **32**(10), 1302–1304 (2007).
5. E. Wikszak, J. Thomas, J. Burghoff, B. Ortaç, J. Limpert, S. Nolte, U. Fuchs, and A. Tünnermann, "Erbium fiber laser based on intracore femtosecond-written fiber Bragg grating," Opt. Lett. **31**(16), 2390–2392 (2006).
6. E. Wikszak, J. Thomas, S. Klingebiel, B. Ortaç, J. Limpert, S. Nolte, A. Tünnermann, and "Linearly polarized ytterbium fiber laser based on intracore femtosecond-written fiber Bragg gratings," Opt. Lett. **32**(18), 2756–2758 (2007).
7. A. Martinez, M. Dubov, I. Khrushchev, and I. Bennion, "Direct writing of fiber Bragg gratings by femtosecond laser," Electron. Lett. **40**(19), 1170–1172 (2004).
8. N. Jovanovic, A. Fuerbach, G. D. Marshall, M. J. Withford, and S. D. Jackson, "Stable high-power continuous-wave Yb^{3+}-doped silica fiber laser utilizing a point-by-point inscribed fiber Bragg grating," Opt. Lett. **32**(11), 1486–1488 (2007).
9. N. Jovanovic, M. Aslund, A. Fuerbach, S. D. Jackson, G. D. Marshall, and M. J. Withford, "Narrow linewidth, 100W cw Yb^{3+}-doped silica fiber laser with a point-by-point Bragg grating inscribed directly into the active core," Opt. Lett. **32**(19), 2804–2806 (2007).
10. N. Jovanovic, J. Thomas, R. J. Williams, M. J. Steel, G. D. Marshall, A. Fuerbach, S. Nolte, A. Tünnermann, and M. J. Withford, "Polarization-dependent effects in point-by-point fiber Bragg gratings enable simple, linearly polarized fiber lasers," Opt. Express **17**(8), 6082–6095 (2009).
11. M. L. Åslund, N. Nemanja, N. Groothoff, J. Canning, G. D. Marshall, S. D. Jackson, A. Fuerbach, and M. J. Withford, "Optical loss mechanisms in femtosecond laser-written point-by-point fibre Bragg gratings," Opt. Express **16**(18), 14248–14254 (2008).
12. D. S. Starodubov, V. Grubsky, and J. Feinberg, "Efficient Bragg grating fabrication in a fiber through its polymer jacket using near-UV light," Electron. Lett. **33**(15), 1331–1333 (1997).
13. J. Jaspara, M. Andrejco, and D. DiGiovanni, "Effet of heat and H2 gas on the photo-darkening of Yb3+ fibers," in Conference of Lasers and Electro-Optics CLEO Technical Digest (OSA, 2006), CTuQ5.

#115071 - $15.00 USD Received 30 Jul 2009; revised 15 Sep 2009; accepted 18 Sep 2009; published 5 Oct 2009

14. M.-A. Lapointe, and M. Piché, "Linewidth of high-power fiber lasers," Proc. of SPIE, Photonics North, (2009)
15. M. Bernier, Y. Sheng, and R. Vallée, "Ultrabroadband fiber Bragg gratings written with a highly chirped phase mask and infrared femtosecond pulses," Opt. Express **17**(5), 3285–3290 (2009).

1 Introduction

The refractive index change resulting from the nonlinear interaction of focused femtosecond pulses (*fs*) with glasses turned out to be a very promising alternative to the defect-resonant UV-induced physical process, which is commonly used for writing fiber Bragg gratings (FBGs) in silica fibers [1-2]. Advantages of the FBG written with *fs* pulses include, among the others: higher erasure temperature, larger refractive index change and possibility to write gratings in non-photosensitive and non-silica fibers. Accordingly, the use of infrared *fs* pulses with a phase-mask was shown as the sole alternative to write efficient FBGs in both doped and undoped fluoride fibers [3]. Such achievement has paved the way to the demonstration of the first monolithic fiber laser made from a fluoride glass fiber [4]. FBGs written with the scanning phase-mask technique using IR *fs* pulses also proved to be crucial for the development of silica fiber lasers doped with either erbium or ytterbium active ions [5,6]. In [6], a maximum output power of 100 *mW* at 1040 *nm* was obtained from an ytterbium-doped panda-type fiber with a laser slope efficiency of 27%. The second-order FBGs involved in this experiment had peak reflectivities of 65% and 45% for each polarization. Another emerging technique to write FBGs in non-photosensitive fibers is the point-by-point (PbP) technique. It employs on a tightly focused spot of the *fs* pulses at 800 *nm* and a high precision positioning stage [7]. Using this technique, a third order FBG with a peak reflectivity estimated to be 90% was inscribed directly in a ytterbium doped double-clad fiber and the laser operation of 5*W* at 1080 *nm* with a slope efficiency of 46% was first reported [8] before the power was eventually scaled up to 100*W* with a slope efficiency of 64% [9]. The PbP technique recently reported to induce high birefringence in the fiber caused by the formation of micro-voids at each exposure spot [10]. Such birefringence was found useful for single polarization emission of the ytterbium fiber laser without the need for external bulk components. However, the PbP writing technique was also reported to introduce strong and permanent optical losses at short wavelengths, which were associated with the optical damage. This will limit somehow applications of the PbP written FBGs, namely in the core pumping configurations [11].

In this paper, we report what we believe is the first demonstration of a fundamental order Bragg grating written directly in a non-photosensitive double-clad ytterbium doped silica fiber. It is accomplished with 400 *nm fs* pulses and a phase-mask. The refractive index modulation in excess of $4\text{x}10^{-3}$ was induced in the fiber core along with large photodarkening losses during the grating formation. Subsequently, the losses were removed by thermal annealing, resulting in a low loss (<0.1*dB*), stable and high reflectivity (>40dB) FBGs. Based on this FBG we demonstrate a fiber laser with a slope efficiency of 71% and a maximum output power of 13*W*, which was only limited by the pump power.

2. Experiment

A Ti-sapphire regenerative amplifier system (Coherent Legend-HE) that produces *fs*-laser pulses of 3.5 *mJ* per pulse at 1 *kHz* repetition rate with central wavelength λ=806 *nm* was used as pump source. The duration of the Fourier-transform limited pulses was measured to be ~35 *fs* using a single-shot autocorrelator. A BBO crystal (Eksma Optics, BBO-1502) was used to produce the second harmonic at 403 *nm* with maximum energy of 1.0 *mJ*. A dichroic mirror was used to separate the 403 *nm* beam from the residual 806 *nm* pump. The 403 *nm* laser beam (resized to ~8.5 *mm* x 15 *mm* at $1/e^2$) was then focused by a cylindrical lens and through a silica phase mask down to a focal line parallel to the fiber core. Based on Gaussian beam optics, the width of the focal line is estimated to be $1.27f\lambda/D$ ~7 μm, where f =112 *mm* is the focal length and D is the beam size perpendicular to the fiber at the focusing lens. In order

#115071 - $15.00 USD Received 30 Jul 2009; revised 15 Sep 2009; accepted 18 Sep 2009; published 5 Oct 2009

to ensure a uniform index modulation over the fiber core the focusing lens was made to oscillate in the transverse direction using a piezoelectric mount, so that the focal line scanned over a 20 μm distance centered on the fiber core at a frequency of 0.05Hz. The fiber to phase-mask separation was set to 3 *mm* in order to prevent damage to the later.

The phase-mask used in the experiment had a uniform pitch of 738 *nm* over a length of 40 *mm*. The phase mask was fabricated in-house by holographic lithography process with an etching depth of 475 *nm* and a duty-cycle of 40% on a UV-grade fused silica substrate. It was designed according to diffraction theory using the rigorous coupled-wave analysis (RCWA), such that under our writing conditions with the wavelength of 400 *nm* and the phase-mask pitch of 738 *nm*, only three diffraction orders (0, ±1) were produced with 3.4% of the energy in the zero order and the remaining 96% in the ±1 orders, thus efficiently contributing to the interference pattern. Transmission and reflection spectra of the FBGs were measured using a super-continuum source (Koheras SuperK Power), an optical fiber coupler and an optical spectrum analyzer (ANDO AQ6317B).

The fiber laser configuration is presented in Fig. 1. The ytterbium doped fiber was a double cladding singlemode fiber with 6μm/128μm core/1stcladding diameters and 0.12/0.46 core/1stcladding numerical apertures. The fiber was co-doped solely with 2 mol% of Al_2O_3, i.e. no extra photosensitive element such as germanium was introduced in the fiber glass matrix. The polymer coating of the fiber was removed prior to writing the FBG but others have shown that it is possible to write through the polymer jacket using near-UV light [12]. In future work, we will attempt to do so because the stripping and recoat process could affect the quality of the fiber. The ytterbium fiber was pumped contra-directionnally using a 2+1->1 multimode pump combiner (ITF Labs MMC0211C2772) made on a matching undoped double cladding fiber (CorActive's Rel-Un-06-02). A matching single cladding fiber was spliced at the output (CorActive's Si-12-06) as a cladding light stripper to make sure only the signal propagating in the core of the fiber was measured with the thermopile (Gentec UP19K-H5) at the output. The high reflectivity (HR) FBG was written directly at one end of a roll of 25 *m* of the doped fiber. The Yb doped fiber was pumped with up to 20W pump power at 915 *nm* from a fiber-coupled pump module (Fianium, PUMA) spliced in one branch of the pump combiner. In one cavity end, a straight cleave was used as a low reflectivity coupler for output of the fiber laser. In the other cavity end beyond the high reflectivity (HR) FBG, the fiber was cleaved to 8 degree in order to prevent any detrimental feedback. Fusion splices were carefully and actively monitored with a stable light source at 1310 *nm* (HP 83437A) and a power meter (ILX FPM-8210H) to maintain losses below 0.1 dB per splice.

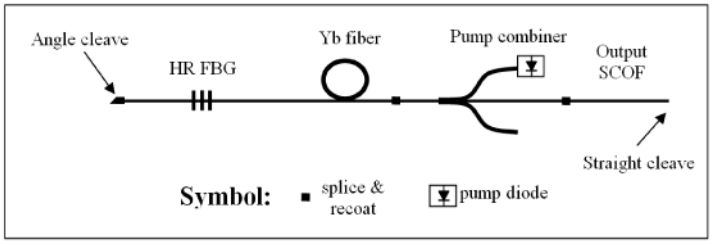

Fig. 1. Ytterbium fiber laser configuration used to test the laser operation incorporating an integrated FBG as a high reflector.

3. Results and discussion

We first exposed for 20 *s* the focused *fs* pulse beam to a length of 15 *mm* of the double-clad ytterbium doped fiber. The reflection and transmission spectra of the resulting FBG are shown in Fig. 2.

#115071 - $15.00 USD Received 30 Jul 2009; revised 15 Sep 2009; accepted 18 Sep 2009; published 5 Oct 2009

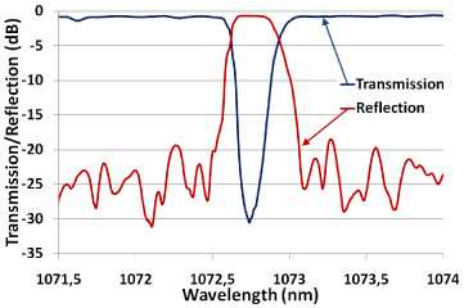

Fig. 2. Measured transmission and reflection spectra of a FBG written in the doped fiber over 15 *mm* at 0.9 mJ, 1 *kHz*, during 20 *s*

A transmission dip of −30 *dB* (corresponding to a reflectivity of 99.9%) is obtained at 1072.7 *nm* with full-width half-maximum (FWHM) of 0.30 *nm*. The throughput (or gray) losses were measured to be 0.6 *dB* using a cut-back at 1075 *nm.* In order to estimate the FBG parameter values, a numerical simulation using *IFO gratings 4.0*^{TM} was performed to fit the experimental spectral curves presented in Fig. 2. The corresponding grating parameters are as follows: grating length = 6.9 *mm*, Gaussian apodization (taper size = 0.5), refractive index modulation = 9.4 x10^{-4}. In order to augment further the FBG reflectivity, we exposed under the same experimental conditions but for twice exposure time of 40 *s* the focused *fs* pulse beam to another piece of the same fiber. The transmission spectrum of the resulting FBG is shown in Fig. 3 (blue curve).

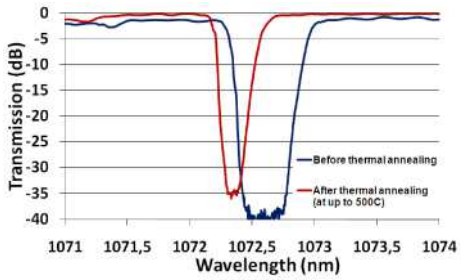

Fig. 3. Measured transmission spectrum of a FBG written in the doped fiber over 15mm at 0.9 mJ, 1 kHz, during 40s before and after thermal annealing at up to 500°*C*.

In this case, a transmission dip < −40 *dB* was obtained with a full-width half-maximum (FWHM) of 0.65 *nm*. Note that the measurement was limited to −40dB due to the limited dynamic range of the characterization set-up. The throughput losses were measured to be 1.2 *dB* and the corresponding refractive index modulation was estimated as 2.1x10^{-3}. This FBG was then thermally annealed in a specially designed oven, where the temperature was increased stepwise by 50°*C* for every 30 minutes ranging from 50 °*C* to 500 °*C*. The resulting transmission spectrum is shown in Fig. 3 (red curve) along with the transmission curve prior to thermal annealing. A 0.2 *nm* spectral shift of the transmission peak is observed along with a narrowing of the peak (FWHM of 0.41 *nm*), and a decrease of the peak reflectivity down to R~-35dB. The most interesting feature resulting from the complete thermal annealing treatment is that the throughput losses could be reduced to less than 0.05 *dB* with a corresponding refractive index modulation of 1.45x10^{-3}. In the thermal annealing process the refractive index change and the corresponding photo-induced fiber background losses in the FBG were carefully monitored as a function of the temperature. Accordingly, for every 30 minutes of annealing treatment at a constant temperature, the FBG transmission spectrum was measured from which the refractive index modulation could be inferred. The evolution of the

#115071 - $15.00 USD Received 30 Jul 2009; revised 15 Sep 2009; accepted 18 Sep 2009; published 5 Oct 2009

refractive index modulation as a function of annealing temperature is shown in Fig. 4 (blue curve) along with the fiber throughput losses evaluated at 1075 *nm* (red curve).

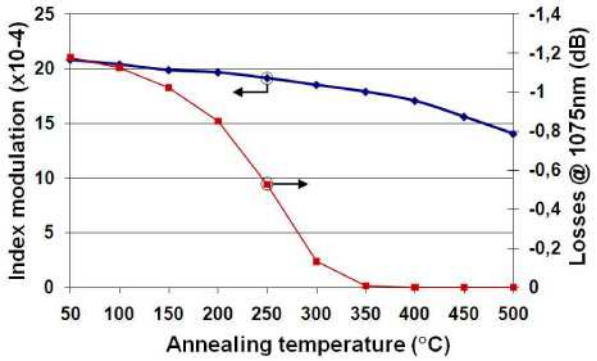

Fig. 4. Evolution of the refractive index modulation (blue) and throughput losses (red) of the FBG introduced at Fig. 2 as a function of the annealing temperature. The corresponding refractive index modulation was evaluated under adiabatic conditions, i.e. after 30 minutes of annealing at the corresponding temperature.

One first notes a slight and almost linear decrease of the refractive index modulation for temperatures up to 350 °*C*. Meanwhile, the throughput losses at 1075 *nm* are shown to decrease essentially to zero as a result of thermal annealing which is consistent with a previous report [13]. This is not surprising since the color centers are destroyed in silica glass above 350-400 °*C*. Consequently, the refractive index change initially resulting from both color center and glass densification would only rely on glass densification following the thermal annealing temperature beyond 350 °*C*. Interestingly, this glass densification contribution to the photo-induced refractive index change seems to be related to negligible photo-induced losses at 1075 *nm*. From a practical viewpoint, a complete recovery of the fiber transmission pristine conditions, that is prior to exposure to the focused *fs* beam, can be obtained by only a few minutes of annealing at 400 °*C*. We tested the annealed FBG shown in Fig. 3 (red curve) as high reflector in the fiber laser configuration previously described. Figure 5 shows the power of the fiber laser as a function of the launched pump power at 915 *nm*.

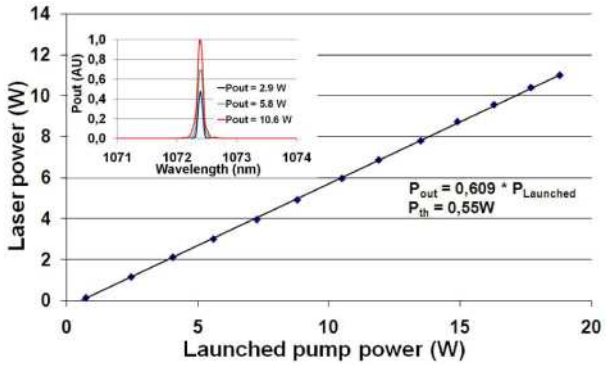

Fig. 5. Measured laser power as a function of the launched pump power when the laser is incorporating the annealed Bragg grating presented in Fig. 3. The inset shows the power spectrum of the laser for different output power of the fiber laser.

Emission spectra for output power levels of 2.9 *W*, 5.8 *W* and 10.6 *W* are also shown in Fig. 5 (inset), confirming that the FBG is efficiently driving the laser emission as expected. The corresponding emission linewidths (FWHM) are 86 *pm*, 103 *pm* and 108 *pm* respectively.

#115071 - $15.00 USD Received 30 Jul 2009; revised 15 Sep 2009; accepted 18 Sep 2009; published 5 Oct 2009

To further confirm the efficiency of the FBG thermal annealing treatment, the fiber was imaged in the vicinity of the FBG using a high resolution thermal camera (VarioCAM Jenoptik) during the laser operation. We did not detect any local variation of the temperature in the vicinity of the FBG, but a rather uniform 6 °C temperature increase over the length of the fiber at the maximum output power instead, thus confirming that no absorption was induced by the thermally annealed FBG. Without such a thermal annealing, we observed that the temperature increase could reach 50 °C in the vicinity of the HR FBG at maximum output power. We also noted that for increasing power, the spectral broadening induced by four-wave mixing is such that the intracavity signal spectrum exceeds the FBG bandwidth significantly, resulting in spectral filtering of the signal [14]. In reducing the actual or effective reflectivity of the HR FBG, this phenomenon contributes to limit the laser efficiency to 61% as shown in Fig. 5. To overcome this limitation, we inscribed a stronger and therefore broader FBG. Figure 6 shows the transmission spectrum of such a FBG written under the same experimental conditions except for an exposure time of 100 *s*.

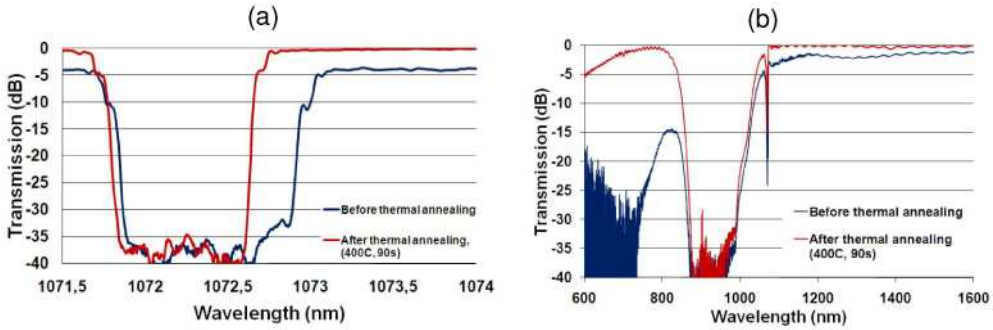

Fig. 6. a) Measured transmission spectrum of a FBG written in the active fiber over 15mm at 0.9 mJ, 1kHz, during 100s before and after a thermal annealing process at 400°C during 90 seconds. b) Corresponding broadband fiber transmission spectrum before and after a thermal annealing at 400°C during 90 seconds.

The effects of the thermal annealing treatment on this FBG were measured in two spectral ranges: Fig. 6(a) shows a close-up of the FBG transmission, whereas Fig. 6(b) illustrates broadband fiber transmission and the corresponding loss recovery. In both cases the detection level is limited to ~-40 *dB* by the noise in the characterization set-up. Following the annealing process, the throughput losses at 1075 *nm* (i.e. measured slightly off the Bragg wavelength not to interfere with the FBG transmission) are shown to pass from −4.0 *dB* to −0.13 *dB* whereas the corresponding photo-induced refractive index modulation is maintained to a large value (i.e. $3.6\text{x}10^{-3}$). In the case of Fig. 6(b), the spectral resolution was set to 1 *nm* and the transmission normalization was obtained by using a cutback reference with an undoped fiber having as similar modal content as the ytterbium doped fiber. It is clear from this result that the photo-induced losses can be eliminated after only 90 *s* of annealing at 400 °*C*. It should also be noted that, alternatively, a FBG with a stop band extending over several nanometers could simply be fabricated using a chirped phase mask [15]. This would prevent from overexposing the fiber to the *fs*-beam as we did to obtain the ~1 *nm* broad FBG of Fig. 6.

We tested the broadband FBG as high reflector in a fiber laser cavity. Figure 7 shows the output power of this fiber laser as a function of the launched pump power at 915 *nm*. Emission spectra for three different power levels of 1.5 *W*, 6.1 *W* and 13.3 *W* are also shown as inset to Fig. 7. The corresponding emission linewidths (FWHM) are now approximately 50 *pm*, 270 *pm* and 500 *pm* respectively. A modulation clearly appears in the shape of the output spectrum at maximum power. Also recall that the spectral width was clamped to ~100 *pm* in the previous configuration (Inset to Fig. 5).

#115071 - $15.00 USD Received 30 Jul 2009; revised 15 Sep 2009; accepted 18 Sep 2009; published 5 Oct 2009

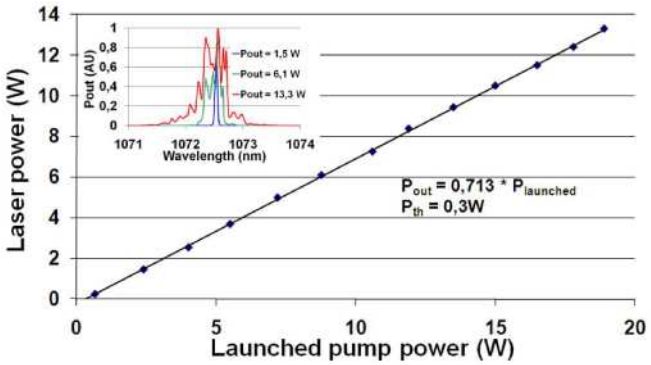

Fig. 7. Measured laser power as a function of the launched pump power at 915 *nm* when the laser is incorporating the annealed Bragg grating presented in Fig. 6. The inset shows the power spectrum of the laser for three output power.

This spectral broadening appears in the output signal because the FBG is now broad enough to reflect it back to the cavity front end. In the previous configuration involving a narrowband high reflector, the new spectral components that were generated by four-wave mixing were outside the reflecting band of the high reflector and therefore leaking through it [14]. This was checked by measuring the power at 1073 *nm* exiting from the HR-FBG end of the cavity. Power in excess of 1 *W* was actually found to leak from this end at the maximum pumping, therefore reducing by ~10% the output power measured from the nominal output end. This essentially explains the improved performance of the laser with an increase in laser efficiency from 61% to 71% and a decrease of the laser threshold from 0.55 *W* to 0.3 *W*. Note that the 71% slope efficiency is approaching the theoretical limit of the ytterbium system when subtracting the residual pump power and the signal and pump insertion losses. No sign of saturation in the laser characteristic curve appears in Fig. 7, so that the output power is truly limited by the available pump power.

4. Conclusion

In summary, the inscription of efficient Bragg gratings using 400 *nm fs* pulses was successfully demonstrated in non-photosensitive ytterbium-doped double-clad silica fibers. The inscription process induces both a refractive index modulation in excess of $4x10^{-3}$ and large photodarkening losses of the active fiber. The latter were removed by thermal annealing. A low loss (<0.1 *dB*), stable and high reflectivity (>40 *dB*) FBG results. The FBG was used as high reflector in a fiber laser cavity. A slope efficiency of 71% with respect to launched pump power is reported with more than 13 *W* of output power at 1072 *nm*, limited by the pump power and the quantum efficiency of the system. We believe that this demonstration will pave the way to the development of splice-less ytterbium doped fiber lasers and other applications where photo-inscription of non-photosensitive material is required.

Acknowledgment

This research was supported by the Canadian Institute for Photonic Innovations (CIPI), the Fonds Quebecois de Recherche Nature et Technologies (FQNRT), the Natural Sciences and Engineering Research Council of Canada (NSERC) and the Canadian Foundation for Innovation (CFI)

#115071 - $15.00 USD Received 30 Jul 2009; revised 15 Sep 2009; accepted 18 Sep 2009; published 5 Oct 2009